PAPER • OPEN ACCESS

Critical vacancy density for melting in two-dimensions: the case of high density Bi on Cu(111)

New Journal of Physics

The open access journal at the forefront of physics

Deutsche Physikalische Gesellschaft **DPG**

IOP Institute of Physics

Published in partnership with: Deutsche Physikalische Gesellschaft and the Institute of Physics

CrossMark

OPEN ACCESS

PAPER

Critical vacancy density for melting in two-dimensions: the case of high density Bi on Cu(111)

Raoul van Gastel[1,4], Arie van Houselt[1,4], Daniel Kaminski[2,3], Elias Vlieg[2], Harold J W Zandvliet[1] and Bene Poelsema[1]

1   Physics of Interfaces and Nanomaterials, MESA+ Institute of Nanotechnology, University of Twente, PO Box 217, 7500AE Enschede, The Netherlands
2   Radboud University, Institute for Molecules and Materials, Heyendaalseweg 135, 6525 AJ Nijmegen, The Netherlands
3   Marie Curie Sklodowska University, Dept. Chem, PI Marii Curie Sklodowskiej 2, PL-20031 Lublin, Poland
4   These authors contributed equally.

E-mail: b.poelsema@utwente.nl

Abstract

The two-dimensional melting/solidification transition of the high density [2012] phase of Bi on Cu(111) has been studied by means of low energy electron microscopy (LEEM). This well defined phase has an ideal concentration of one Bi atom per two Cu surface atoms ($\theta_{Bi} = 0.500$). The Bi density is determined accurately *in situ* and the highest melting temperature of 538 K occurs at exactly $\theta_{Bi} = 0.500$. A significantly reduced melting temperature is observed for lower Bi densities ($\theta_{Bi} < 0.500$) and, surprisingly, also for $\theta_{Bi} > 0.500$. At $|\Delta \theta_{Bi}| = 0.015$ the melting temperature is reduced by about 20 K. This lowering of the melting temperature is attributed to a critical vacancy density at melting and we propose that this quantity triggers the 2D solid–liquid phase transition. For this particular system, the critical vacancy fraction for melting amounts to 5%–6%. Above $\theta_{Bi} = 0.500$ and near melting a homogeneous, unilaterally compressed phase, '[2012]' is observed, with a density that increases continuously with coverage. It is commensurate along $\langle 11\text{-}2 \rangle$ and incommensurate along $\langle 1\text{-}10 \rangle$. The ability to distinguish between Bi accommodated within the '[2012]' phase and Bi residing on top as a lattice gas by applying LEEM is of crucial importance for the analysis.

Introduction

The two-dimensional melting transition was coined controversial already in 1988 by Strandburg in her comprehensive review [1]. The field is strongly dominated by theory, but 2D melting is still not understood in detail after a few more decades as established by Gasser *et al* [2]. We attribute this to a lack of sufficient and relevant experimental data. Melting in, e.g., colloidal systems with particle sizes of about 4.5 μm [3] and macroscopic air-fluidized modular granular systems [4] have been reported. However, except for classical systems, mainly condensed noble gas layers (see e.g. [1] and references therein), studies of 2D melting in atomic scale systems are still rare. Where noble gas layers show attractive (Van der Waals) forces we concentrate here on a high density atomic scale system with (strong) repulsive interactions: Bi/Cu(111).

Bi surface alloys and ultra-thin Bi films on the Cu(111) substrate have shown a rich mixture of various physical effects [5–9], including order–disorder transitions [6], a gradual de-alloying [5], and even a liquid-to-lattice gas phase transition [5]. One of the effects that was predicted in the phase diagram of the Bi/Cu(111) system after the original structure determination [8], was the occurrence of a Bi coverage dependent melting temperature of the [2012] overlayer phase which forms in this system. Here we study the melting behavior of solids in two-dimensions, as observed through the coverage dependence of the melting of 2D [2012] Bi on Cu(111). When Bi is deposited on Cu(111) at temperatures around 400 K, it initially forms a well-ordered surface alloy with a ($\sqrt{3} \times \sqrt{3}$)-R30^0 structure. Upon exceeding a Bi coverage of 1/3 ML this surface alloy phase

is replaced by an adsorbed phase, the unit cell of which is described by a [2012] matrix [8, 10]. This phase completely covers the visible surface from $\theta_{Bi} \approx 0.47$ ML, i.e. closely below its ideal Bi coverage, θ_{Bi}, of 0.500 ML. This allows us to monitor the melting transition of the [2012] phase in a narrow coverage range around 0.50 ML to visualize the effects of its incomplete structure and associated artificially elevated vacancy density below 0.500 ML, and to understand the effects of stress and strain above 0.500 ML. A vacancy is defined as an unoccupied site in the [2012] phase. For the incommensurate phase above ~0.504 a vacancy is defined as a missing atom from the intrinsic compressed phase. This yields new fundamental insight into how each of these physical quantities affects the melting of a solid in two-dimensions.

Experimental details

A Cu(111) surface[5] was prepared by cycles of 1 keV Ar$^+$ ion bombardment and annealing to 1100 K until good quality LEED patterns were obtained and no contaminations were detected with Auger electron spectroscopy. The nominal orientation was approximately 0.1° (see also [11]). The bismuth was evaporated from a Knudsen cell at a rate of 3 monolayers per hour, where a monolayer is defined as one Bi atom per outermost Cu atom. Since this particular run was part of a much longer experiment, it needs to be pointed out that the starting point of the measurements was not a pristine Cu surface, but instead a surface on which various temperature cycles had already been performed. As we have shown in previous publications [7, 8], the Bi will leave behind a range of three-dimensional structures containing Bi, but likely also Cu since they persist to 800 K. The surface under investigation here was prepared by evaporating Bi at an elevated temperature of 410 K and depositing more Bi after several temperature cycles had already been performed. The 3D structures are therefore stable remnants of previous experimental runs. In view of their complete stability at temperatures up to even 800 K and the comparatively minute temperature variations in the experiment described here, we infer that they do not affect the total Bi coverage.
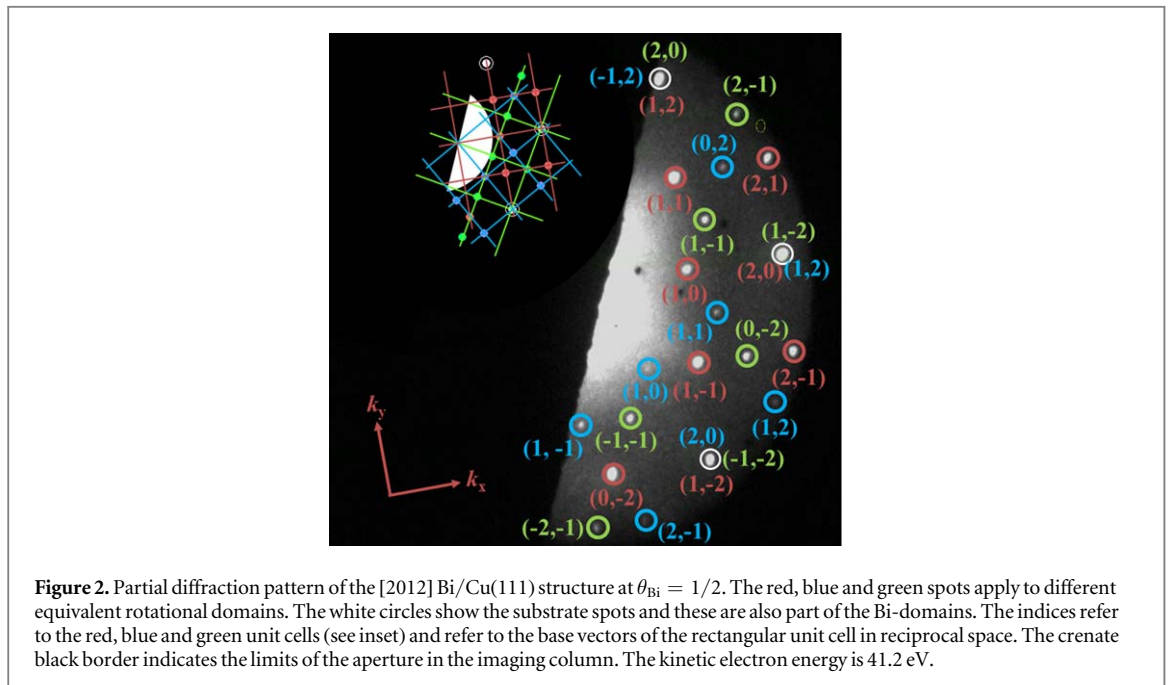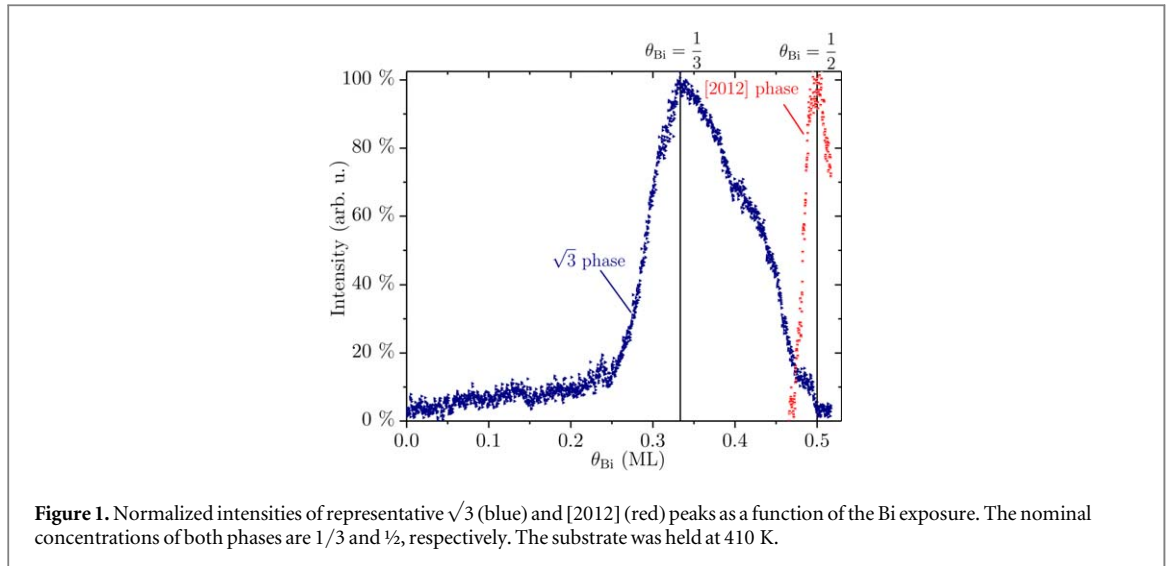
The melting of the [2012]-phase was monitored by recording bright-field low energy electron microscopy (LEEM) images with a slightly tilted beam. The [2012]-phase consists of three equivalent rotational domains. In a well-aligned bright-field image, each of the three phases contributes equally to the total reflected intensity. With a slightly tilted beam, this is no longer the case and three different gray levels can be observed in the images. When the [2012]-layer is subsequently molten, the three rotational domains no longer exist and yield a single uniform gray level. The melting transition can therefore simply be monitored by observing the number of gray levels in the LEEM images.

The temperature was measured with a thermocouple and the readings were calibrated against those underlying the earlier measurements [8, 9]. The relative accuracy is estimated at 0.2 K, while the absolute one may be off by <10 K.

Calibration bismuth coverage and the structure beyond a coverage of 1/2
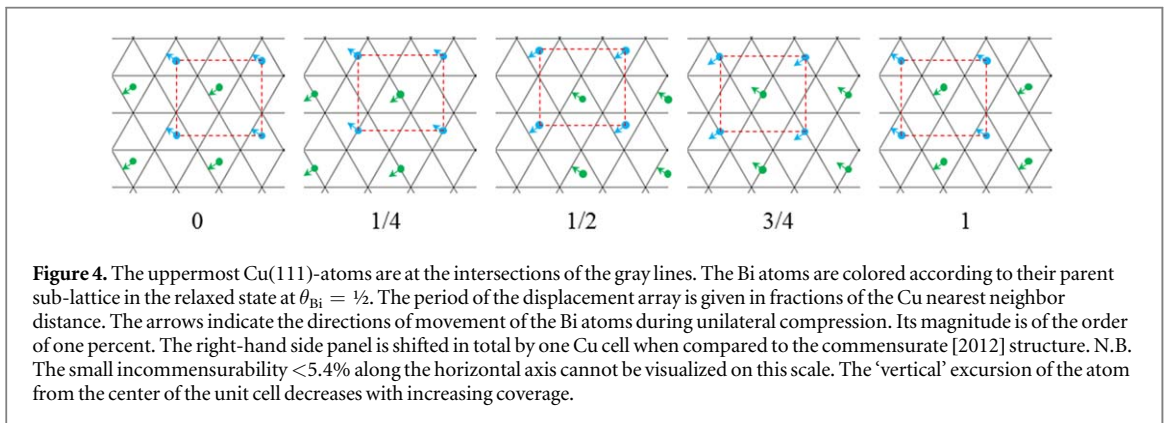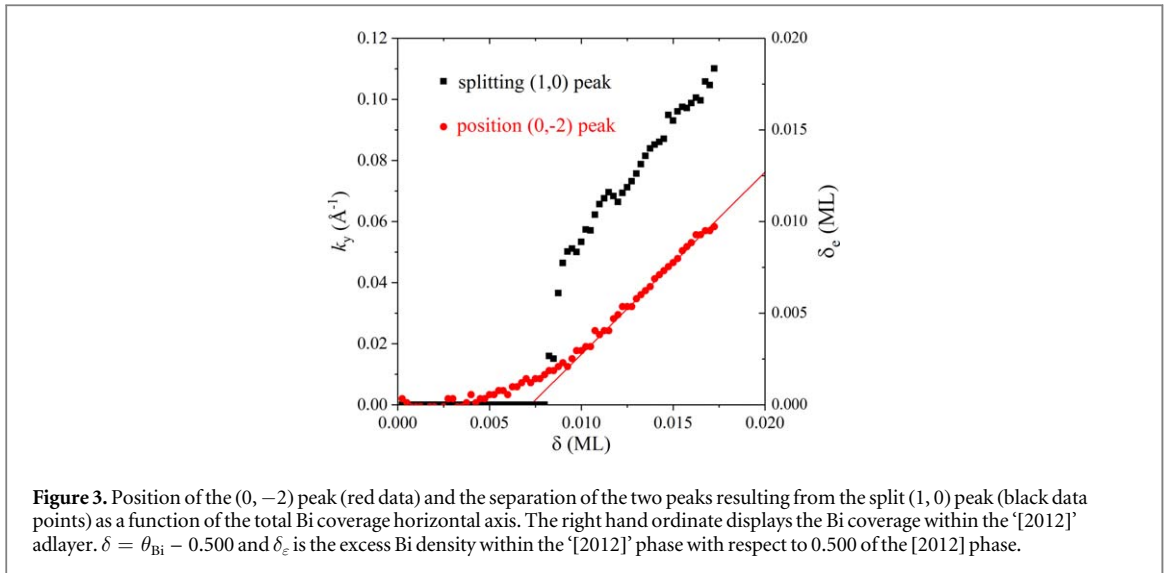
Upon deposition of Bi on Cu(111) at $T = 410$ K a surface confined substitutional alloy with a $(\sqrt{3} \times \sqrt{3})R30°$ structure is formed initially, which culminates at a coverage $\theta_{Bi} = \frac{1}{3}$. Above this coverage the visible area fraction of the alloy is continuously reduced and the Bi atoms form an added [2012] superstructure, which is completed at $\theta_{Bi} = \frac{1}{2}$ and appears in three equivalent orientations. Figure 1 shows relative peak heights of representative peaks of the $\sqrt{3}$- and of the [2012]-structure, in blue and red, respectively. The $\sqrt{3}$ peak appears quite late, which indicates repulsive interactions between the embedded Bi atoms, and it has a well defined maximum intensity at $\theta_{Bi} = \frac{1}{3}$. The [2012] peak also emerges late, equally indicative of repulsive interactions between the adsorbed Bi atoms. No evidence of the crystalline [2012] phase is found below $\theta_{Bi} = 0.47$. The distinct peak is well defined and exhibits a sharp maximum at $\theta_{Bi} = \frac{1}{2}$. The position of the narrow peak of the [2012] phase allows to estimate the absolute coverage with an accuracy of 0.001. The maximum of the $\sqrt{3}$ phase occurs at exactly 1/3 as expected. We emphasize that the substitutional Bi structure at $\frac{1}{3}$ coverage completely disappears in favor of the [2012] Bi ad-structure at $\theta_{Bi} = \frac{1}{2}$ coverage. No alloying is present beyond $\theta_{Bi} = \frac{1}{2}$ due to the large Van der Waals size of Bi compared to Cu. The latter agrees with the findings for Ag/Pt(111) [12, 13], in line with the generic explanation given by Tersoff [14]. Figure 2 shows part of the corresponding diffraction pattern obtained using LEEM. In order to show all three domains, many peaks have been overexposed on purpose. The peaks encoded with different colors correspond to each of the three equivalent rotational domains. The indices refer to the peaks of the [2012]-structure, while also three first order substrate peaks are encircled in white. The positions of the colored peaks vary with increasing total Bi-coverage between 0.50 and 0.518 as can also be observed by carefully considering the attached movie is available online at stacks.iop.org/NJP/20/083045/mmedia: they move along $\langle 1\text{-}10 \rangle$ directions at the Cu(111) surface. As concluded already from x-ray diffraction data [8], the Bi atoms form a [2012] structure with a rectangular unit cell at $\theta_{Bi} = \frac{1}{2}$. The central Bi-atom is off-center and quite close to a hcp position on the

---

[5] The crystal was prepared by Surface Preparation Laboratory, The Netherlands.

Figure 1. Normalized intensities of representative $\sqrt{3}$ (blue) and [2012] (red) peaks as a function of the Bi exposure. The nominal concentrations of both phases are 1/3 and ½, respectively. The substrate was held at 410 K.

Figure 2. Partial diffraction pattern of the [2012] Bi/Cu(111) structure at $\theta_{Bi} = 1/2$. The red, blue and green spots apply to different equivalent rotational domains. The white circles show the substrate spots and these are also part of the Bi-domains. The indices refer to the red, blue and green unit cells (see inset) and refer to the base vectors of the rectangular unit cell in reciprocal space. The crenate black border indicates the limits of the aperture in the imaging column. The kinetic electron energy is 41.2 eV.

Cu(111) surface. It is actually shifted from this position towards the center of the unit cell. We find that this shift increases continuously with increasing total Bi coverage. The resulting single, incommensurate, unilaterally compressed phase is referred to as '[2012]'.

Figure 3 shows the position of the $(0, -2)$ peak as a function of the total Bi coverage, δ, in excess of 0.50 along a $\langle 1\text{-}10 \rangle$-direction in real space, i.e. along the long axis of the rectangular unit cell. The shift of this peak is a direct measure of the in-plane density of Bi (δ_e, right hand scale) in the three equivalent domains. We stress that the compression of Bi within the '[2012]' domains only starts after δ passes a certain limit ($\delta \geqslant 0.007$). This is attributed to the initial formation of a Bi lattice gas on top of the '[2012]' domains. This also explains the swift decay of the intensity of the diffraction peak representing '[2012]' (see figure 1) for $\theta_{Bi} > 0.500$. This decay is a direct consequence of diffuse scattering from the Bi lattice gas building up on top of the '[2012]' domains [15]. From the occurrence of unilateral compression within '[2012]' domains one must conclude that the Bi atoms prefer to bind to the substrate, as compared to residing on top of '[2012]' patches. These findings lead to a refinement of the proposed phase diagram for Bi/Cu(111). For a coverage beyond $\theta_{Bi} = 0.500$ [8] reports the coexistence of two phases: a commensurate, non centered [2012] phase and a centered phase, UIC, with a local density of 0.527, commensurate along $\langle 11\text{-}2 \rangle$ and incommensurate along $\langle 1\text{-}10 \rangle$. Our actual findings are incompatible with the presence of two coexistent phases for temperatures above 410 K. Instead, we observe upon deposition of Bi at 410 K a single, incommensurate, homogeneous phase with a density that increases

Figure 3. Position of the (0, −2) peak (red data) and the separation of the two peaks resulting from the split (1, 0) peak (black data points) as a function of the total Bi coverage horizontal axis. The right hand ordinate displays the Bi coverage within the '[2012]' adlayer. $\delta = \theta_{Bi} - 0.500$ and δ_ε is the excess Bi density within the '[2012]' phase with respect to 0.500 of the [2012] phase.

Figure 4. The uppermost Cu(111)-atoms are at the intersections of the gray lines. The Bi atoms are colored according to their parent sub-lattice in the relaxed state at $\theta_{Bi} = \frac{1}{2}$. The period of the displacement array is given in fractions of the Cu nearest neighbor distance. The arrows indicate the directions of movement of the Bi atoms during unilateral compression. Its magnitude is of the order of one percent. The right-hand side panel is shifted in total by one Cu cell when compared to the commensurate [2012] structure. N.B. The small incommensurability <5.4% along the horizontal axis cannot be visualized on this scale. The 'vertical' excursion of the atom from the center of the unit cell decreases with increasing coverage.

continuously with Bi coverage. It appears to gradually connect the [2012] at 0.500 and the limiting case, UIC, at 0.527 without a density gap. This '[2012]' phase is stabilized by a low density lattice gas of Bi on top of the first Bi layer.

Compression necessarily leads to a displacement of all Bi atoms from their energetically favored positions within the [2012] structure at $\theta_{Bi} = 1/2$. As a result an energetic barrier exists before compression sets in. The lattice gas acts as an enabler for the unilateral compression. The density of this lattice gas amounts to about 0.0075 Bi atoms per Cu(111) unit cell. Compression starts when the gain in energy for Bi binding directly to the substrate, as compared to binding on top of the '[2012]' phase, exceeds the loss of energy of the Bi atoms when they are forced to leave their optimal binding sites due to compression. Figure 3 also shows data for the (1, 0) peak. This peak splits and shown is the distance between the two components, again along a ⟨1-10⟩ azimuth. The splitting reveals details of the behavior of the '[2012]'-structure during compression and the delayed appearance of the splitting is in line with the formation of a lattice gas on top of the '[2012]'-domains.

In order to understand the compression in more detail we refer to figure 4. It shows a sketch the positions of the Bi atoms. For simplicity we consider a case in which the Bi atoms assume fcc and hcp positions on the Cu(111) surface $\theta_{Bi} = 0.500$. We note that in reality the central atom may be closer to the center of the unit cell and it does approach the center even more closely with increasing Bi coverage [8]. The compression takes place along the horizontal direction, i.e. a ⟨1-10⟩ direction and as a result the atoms move in the direction indicated by the small green and blue arrows. The blue (and also the green) atoms assume identical positions with a period given by $1/\delta_\varepsilon$ in units of the Cu nearest neighbor spacing. This can be seen by comparing the extreme left hand and right hand panels in figure 4 and also its caption. The splitting of the (1, 0) peak is reproduced in a calculation using the kinematic approximation, see figure 5. It becomes immediately clear that the amount of splitting is a direct measure of the amount of Bi *within* the '[2012]' domain. The most direct measurement of the amount in excess of a Bi coverage of ½ is obtained from the position of the (0, −2) peak. The splitting is twice the shift of the (1, ±1) peaks in accordance with the experimental data in figure 3.
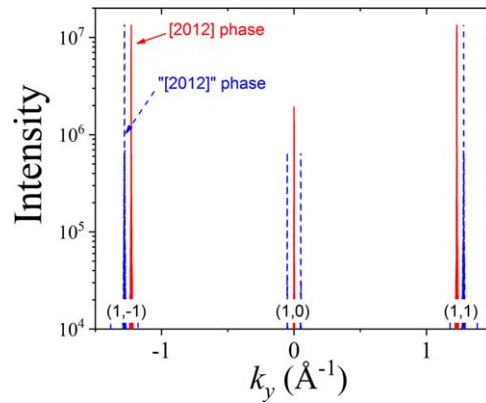
Figure 5. Calculated diffraction patterns along the ⟨1-10⟩ direction in real space and thus along the k_y-axis defined in figure 2. The red and blue curves apply for the commensurate and the unilaterally compressed incommensurate structure, respectively. In the calculation the compression has an assumed value of 4%.
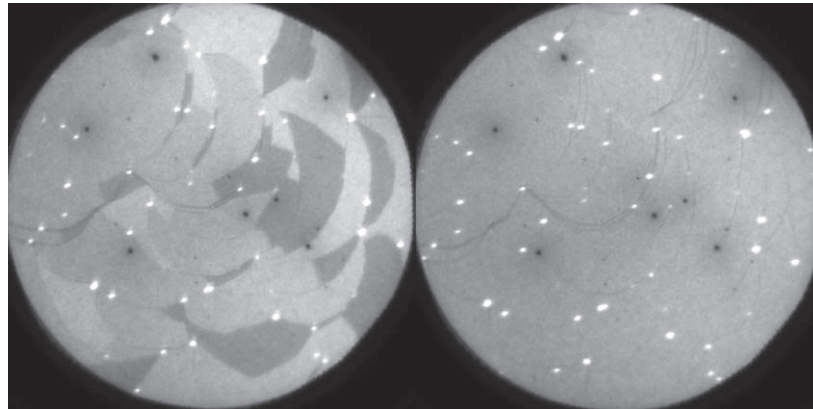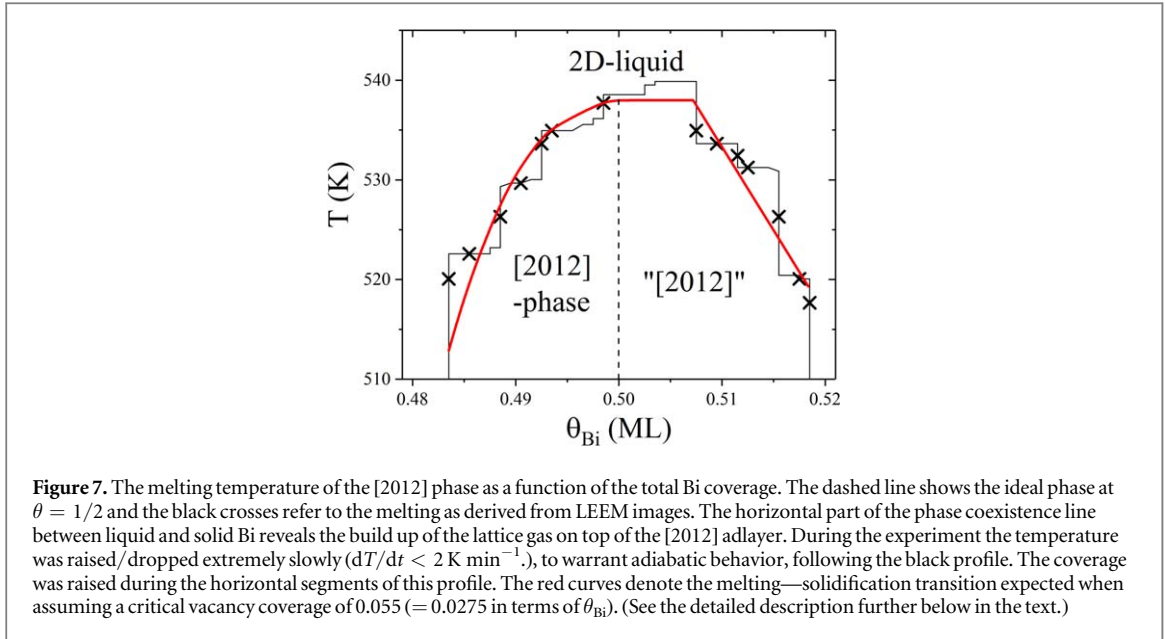

Figure 6. LEEM images just before (left) and just after (right) melting. The three different shades of gray indicate three equivalent rotational [2012] phases. The field of view is 4 μm, the electron energy 6.4 eV and the temperature about 523 K. Step bunches and single steps appear as curved dark lines. The dark spots show defects in the channelplate and the bright spots are stable 3D remnants of previous experimental runs. These are completely stable at 800 K and act as non-participating spectators in the current experiments.

It is also noted that ¼ and ¾ of the period of the compression of the '[2012]' phase, illustrated in figure 4, the local structure becomes a centered one and for those situations the intensity of the (m, n) peaks goes to zero when $m + n$ assumes an odd value. This is the basis of the peak splitting for $m = 1, n = 0$. Indeed the intensity of the $(1, \pm1)$ peaks goes toward a distinct minimum intensity (see the discussion further below and also the movie provided in the added material). In slightly different wording, the glide mirror plane along the horizontal ⟨1-10⟩ direction is in agreement with the missing or clearly reduced intensity for the (m, n) peaks with $m = 0$ and $n = 1, 3, \ldots -1, -3, \ldots$ The residual intensity may be explained by the slightly tilted electron beam.

The melting temperature with variation of the Bi density around $\theta_{Bi} \approx 0.5$

Bi was deposited up to $\theta_{Bi} = 0.483$ ML at 410 K. After reaching this coverage the temperature of the substrate was increased until the melting transition was observed. Figure 6 illustrates how the melting transition of the [2012] phase is identified in bright-field LEEM. The left hand image was taken just before melting.

Each of the three equivalent [2012] domains has a somewhat different gray tone due to a purposely slightly misaligned microscope. These different levels of gray disappear after melting as shown in the right hand image, where no indication for crystalline domains is visible anymore. We note here that the fluctuations of the domain borders are strong just before melting (see the also added second movie). The melting line of the Bi [2012]-phase was then probed by an alternating step-wise increase of coverage and temperature (horizontal and vertical line segments, respectively). The sequence of melting and solidification transitions was continued until upon increasing Bi coverage a solidification was no longer observed within a reasonable timeframe. This behavior is observed for the total Bi coverages exceeding 0.50 ML. The experiment was then continued by changing the sign of the temperature change. Above 0.50 ML the melting and solidification transitions were again observed in an

Figure 7. The melting temperature of the [2012] phase as a function of the total Bi coverage. The dashed line shows the ideal phase at $\theta = 1/2$ and the black crosses refer to the melting as derived from LEEM images. The horizontal part of the phase coexistence line between liquid and solid Bi reveals the build up of the lattice gas on top of the [2012] adlayer. During the experiment the temperature was raised/dropped extremely slowly ($\mathrm{d}T/\mathrm{d}t < 2\,\mathrm{K\,min}^{-1}$.), to warrant adiabatic behavior, following the black profile. The coverage was raised during the horizontal segments of this profile. The red curves denote the melting—solidification transition expected when assuming a critical vacancy coverage of 0.055 (= 0.0275 in terms of θ_{Bi}). (See the detailed description further below in the text.)

alternating fashion, now for a decreasing value of the temperature following the deposition of additional bismuth. The just described direct excursion through the phase diagram of the Bi/Cu(111) system is plotted in figure 7.

Before we address the physics underlying the remarkable coverage dependence of the melting temperature we remind our readers of the fact that melting in three dimensions is accompanied by the appearance of a significant equilibrium density of vacancies within the crystal. At melting, this density can amount to several percent for high melting point metals [16]. This bulk defect concentration, which increases exponentially upon approaching the melting point has been measured by macroscopic methods [16] and also inferred from microscopic experiments [17]. Here we propose that the vacancy density can be used as a criterion for melting in two-dimensions too. Vacancy induced melting was suggested before in literature [18, 19], but not demonstrated quantitatively.

We first focus on the center of the phase diagram. For the ideal [2012] phase the fundamental thermal excitation is the generation of a vacancy-adatom pair, i.e. a Bi atom from the [2012] layer is promoted to a Bi adatom on top of this phase, leaving behind a vacancy. By definition, the fractional coverage of adatoms, θ_a, is identical to that of vacancies, θ_v, given by

$$(1 - \theta_v)(1 - \theta_a)\mathrm{e}^{-\frac{E_v}{k_B T}} = \theta_a \theta_v, \tag{1}$$

$$\theta = \theta_a = \theta_v = \frac{1}{1 + \mathrm{e}^{\frac{E_v}{2k_B T}}}, \tag{1a}$$

where E_v is the formation energy of the vacancy. The left-hand side describes the generation of vacancy adatom pairs. For the generation of these pairs one requires for an excitation at any given lattice site, that the site is filled at the lower level within the adlayer, and not occupied by an adatom at the higher level on top of the adlayer. The right-hand side gives the annihilation of a vacancy by descent of an adatom, which requires an unoccupied site at the lower level and a filled site at the higher level. In equilibrium both sides are equal, giving rise to the result in equation (1a). For a hypothetical case with $E_v = 0$ one arrives at the required result that the probability to fill both levels is equal (1/2). For sake of completeness we mention that, due to mutual interactions between the adsorbed Bi atoms, the formation energy of vacancies may depend on coverage.

For a coverage smaller than $\theta_{Bi} = \frac{1}{2}$ ML we deal with vacancies of non-thermal origin too. Their fractional coverage, V, is determined by the exact exposure at which the Bi flux was stopped before obtaining each individual data point. Near the melting point also vacancies and adatoms are generated thermally with $\theta = \theta_v = \theta_a$. We can safely assume that equilibrium exists between the vacancies within the [2012] layer and the adatoms on top. For the generation and annihilation of vacancy/adatom pairs in equilibrium we find

$$(1 - V - \theta)(1 - \theta)\mathrm{e}^{-\frac{E_v}{k_B T}} = (V + \theta)\theta. \tag{2}$$

Table 1. Forced fractional vacancy coverage, V, and melting temperature, T_m in [2012] phase.

V	0.033	0.029	0.023	0.019	0.015	0.013	0.003	0
T_m (K)	520.0	522.5	526.5	529.5	533.5	535.0	537.5	538.0

Table 2. Compression, $\xi\,(=2\,\delta_\varepsilon)$, and corresponding melting temperature, T_m in '[2012]' phase.

ξ	0	0.003	0.005	0.008	0.011	0.017	0.020	0.022
T_m (K)	538.0	535.0	533.6	532.4	531.3	526.3	520.1	517.7

This gives rise to a 2nd order polynomial in θ

$$(\varphi - 1)\theta^2 + (-2\varphi + V\varphi - V)\theta + (1 - V)\varphi = 0 \tag{3}$$

with $\varphi = \exp(-E_v/k_B T)$ and $V = 2\cdot(0.500 - \theta_{Bi})$. For any given combination of V and (coverage dependent) E_v we obtain the coverage of thermally generated vacancies (=that of adatoms) θ. Entropic effects may be of some (minor) significance, but are ignored here.

The experimentally observed melting temperatures in the presence of non-thermal fractional vacancy concentrations V are summarized in table 1. Note that the melting temperature in the last column is the result of the fit. We now propose that a critical fractional vacancy coverage, $\theta_{vcr} = V + \theta$ triggers melting. To check this presumption we have calculated $V + \theta$ for a number of assumed θ_{vcr}—values using equation (3). We find that the obtained critical fractional vacancy coverage is constant already within $\pm 14\%$ upon a variation of the forced fractional vacancy coverage by an order of magnitude (0.003–0.033).

We now discuss the right-hand side branch of the phase diagram in figure 7. The data are summarized in table 2. We apply the same conjecture that the same constant critical fractional vacancy density θ_{vcr} is required for melting. Since we now are dealing with the intrinsic system (i.e. $V = 0$) equation (1) can be rewritten as

$$E_v(\xi) = 2k_B T_m(\xi) \ln\left(\frac{1}{\theta_{vcr}} - 1\right). \tag{4}$$

As according to table 2 the melting temperature decreases with increasing compression the formation energy of vacancies in the 2D '[2012]' film has to decrease too. Indeed the increasing repulsion within the film leads to a reduced binding of Bi to the substrate and thus a lowering of the formation energy for vacancies E_v. Therefore, the concept of a constant required fractional vacancy concentration which triggers melting provides a viable framework for a consistent explanation of understanding both branches of the phase diagram in figure 7 (see further below).

Discussion

The acquisition time for the data shown in figure 7 has been about 3 h, i.e. $\sim 10^4$ s. In order to keep the system sufficiently stable under these conditions and allow for the applied analysis, the loss of Bi material should be kept below ~ 0.01 ML. The vapor pressure of Bi at the melting point (544 K) equals about 10^{-9} mbar [20]. We first assume that the Bi atoms on top of the [2012] film behave like adatoms on the surface of a bulk Bi crystal. Then the evaporation rate in equilibrium would be compensated by the impingement rate which equals about 10^{-4} per lattice site per second. The estimated loss of material during the experiment is then about the coverage of adatoms. For an adatom fractional coverage of 0.02 the loss of material would be 0.01 ML. Taking into account that most of the time the substrate temperature is below 538 K (see figure 7), we conclude that the mass conservation limits mentioned above are just secured. This implies that the adatom fractional density and thus the critical fractional vacancy coverage for melting, θ_{vcr}, has to be only about a few percent or less. The evaporation from the [2012] phase directly into vacuum must be less than this amount and therefore the binding energy of Bi to Cu(111) must be $\geqslant 1.95$ eV.

We emphasize once more that the melting temperature as a function of the Bi density behaves differently on each side of the ideal coverage $\theta_{Bi} = \frac{1}{2}$ in a *qualitative* sense. Due to a fundamentally different origin of the Bi vacancies in the [2012] phase, as described before, the melting temperature *increases* with increasing θ_{Bi} for $\theta_{Bi} < \frac{1}{2}$ and *decreases with* increasing θ_{Bi} for $\theta_{Bi} > \frac{1}{2}$. The plain fact that we observe this trend reversal at the expected coverage unequivocally implies that the loss of Bi due to evaporation during the experiment is negligible and that the precise Bi coverage can be accurately established.

In conclusion, θ_{vcr} must be (well) above 0.033, the highest applied fractional coverage of non-thermal vacancies used in the experiment. At the same time it probably is smaller than ∼0.06 since we find no stable [2012] phase below $\theta_{Bi} \approx 0.47$ as derived from figure 1. It is tempting to conclude that the [2012] Bi phase below this coverage is molten too. (At least, it shows no long range ordering.) For a possible variation of θ_{vcr} from 0.033 to 0.06 the corresponding vacancy formation energy varies (see equation (4)) from 314 to 255 meV. This result can be compared to 350 meV for the formation energy of bulk vacancies in Bi [21]. Usually the formation energy for surface vacancies is lower than that for bulk vacancies. Polatoglou *et al* [22] found for a number of metals a ratio of 0.58–0.71. The ratio of coordination numbers, as often suggested in statistical physics, would lead to a factor of 0.75. It must be considered here too that the bond strength to Cu(111) is relatively high (see discussion above) which leads to an increase of the formation energy of vacancies within the [2012] layer. It is concluded that the obtained value of 264 meV for the formation of vacancies in the [2012] Bi layer on Cu(111) is reasonable indeed.

From equation (4) and the data in table 2 we derive that the unilateral compression of the '[2012]' phase leads to a linear decay of the formation energy for vacancies with increasing compression ξ

$$E_V(\text{meV}) = 264 - 410\xi. \tag{5}$$

This weak dependence on the compression does not affect the conclusions for stability of the '[2012]' phase as discussed above. The experimental phase coexistence line for the liquid and '[2012]' solid as shown by the right red curve in figure 7 is described well by equations (1), (4) and (5) for $\theta_{vcr} = 0.055$.

As already noted in the discussion of figure 1 the late emergence of the diffraction peaks of the [2012] phase is straightforwardly understood in terms of strong repulsion between bismuth atoms. In the extreme case of a description in terms of a hard honeycomb model [23] the transition from a disordered fluid phase to an ordered crystalline would occur a $\theta_{Bi} = 0.422$. We observe the ordered crystalline phase only for $\theta_{Bi} > 0.47$ which is attributed to repulsion near completion of the [2012] phase. When these (strong) interactions are tentatively described by

$$E_v(\text{meV}) = 264 + 1800\left(\frac{1}{2} - \theta_{Bi}\right) \tag{6}$$

one obtains a nicely *constant* critical vacancy fraction for melting of 0.055. The application of equations (2) and (6) results in the red curve representing the phase existence between liquid Bi and the [2012] solid in the phase diagram in figure 7 (left hand branch).

We conclude that the phase coexistence line between 2D liquid and 2D solids around $\theta_{Bi} = 0.500$ is perfectly described by assuming a single critical vacancy fraction for melting of 0.055. Slightly different values of θ_{vcr} would equally well describe the experimental data. The single data point that is off by a distinct margin is the first one at 520 K. Before measuring this data point the sample temperature was raised over a larger route and the sample temperature probably lacked behind somewhat. A quantitative estimate is considered impossible.

In the present case the system is in essence a two level system in which Bi atoms originating from the lower [2012] layer can be promoted into an adatom site in the higher layer. Establishing equilibrium between the adatoms and the vacancies in these layers requires sufficiently long lifetimes of the adatoms in the higher layer, i.e. loss of atoms to the vacuum (evaporation) should be zero (or negligible). In that case also the formation energy of vacancies should be sufficiently low in order to let them occur before evaporation takes place. The bond strength to the substrate is an important parameter as well. Under these conditions the concept of a critical vacancy density for melting provides a powerful frame work for understanding the reversible melting— solidification behavior. Further experiments are needed to verify whether this simple concept can be helpful in understanding 2D melting more in general. Difficulties such as structural phase transitions within the 2D film, the corrugation of the interaction potential between adsorbate and substrate, as well as attractive interactions between the adsorbates can play an important and deceptive part too. These probably contribute to the deviating behavior reported for Pb/Cu(111) [24].

The elaborate previous paper [8] on this system reports for coverages $\theta_{Bi} > 0.500$ the coexistence of two solid phases, i.e. the limiting incommensurate UIC phase with a local coverage of 0.527 and the also limiting commensurate [2012] phase with a coverage of 0.500. A sketch of both conform unit cells is shown in figure 8. It was also emphasized that the UIC structure is centered and the [2012] is not. The excursion Δ of the central atom along the ⟨11-2⟩ direction (vertical line in figure 8) amounts to 0.54 Å [8]. (For the UIC structure $\Delta = 0$ [8]).

Information on Δ is accessible in our current experiment by analyzing the peak intensities in the recorded LEED patterns, as exemplified in figure 2 and in the accompanying movie. For the centrosymmetric UIC structure ($\Delta = 0$) the (m, n) peaks with odd $(m + n)$ values are forbidden. Within the kinematic approximation the integral area of the $(1, 0)$ peak is then proportional to:
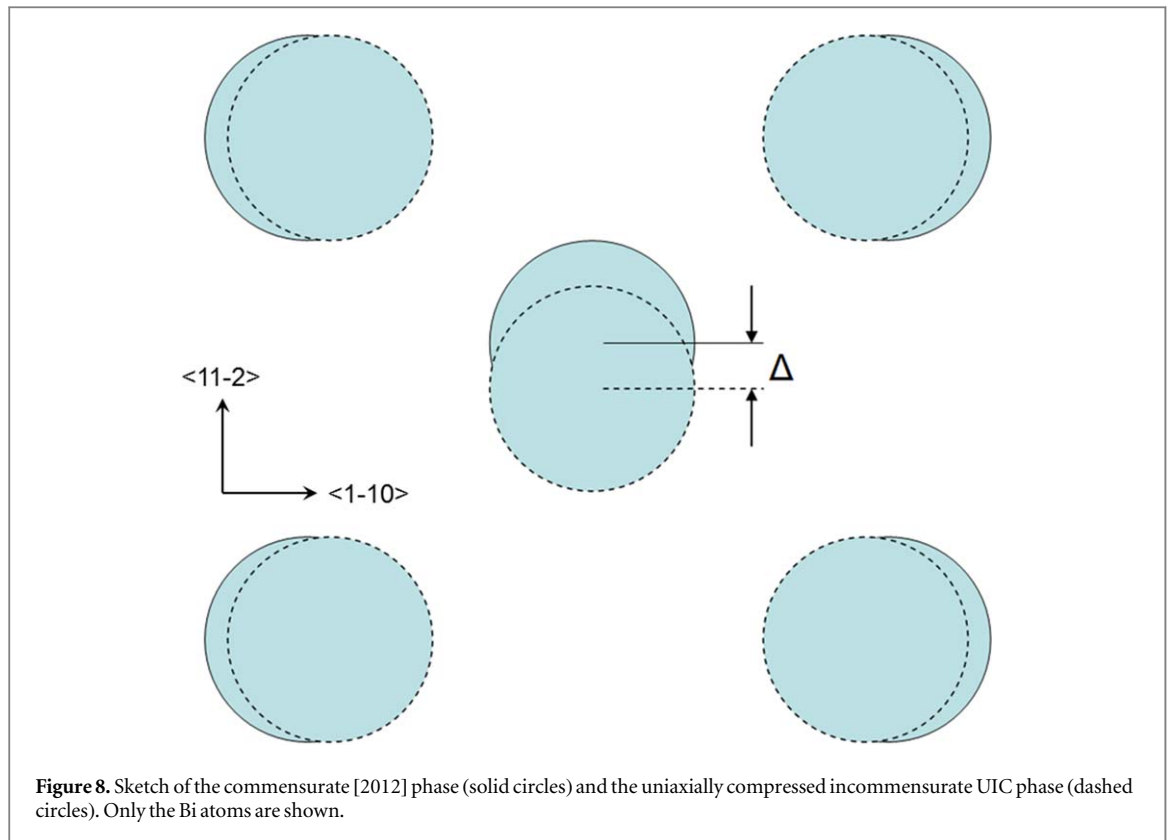
Figure 8. Sketch of the commensurate [2012] phase (solid circles) and the uniaxially compressed incommensurate UIC phase (dashed circles). Only the Bi atoms are shown.

$$I_{10} = 1 + \cos\left(\pi + \frac{2\pi\Delta}{d}\right) = 1 - \cos\left(\frac{2\pi\Delta}{d}\right), \tag{7}$$

where d is the size of the unit cell along ($\langle 11\text{-}2\rangle$) Cu rows. For the symmetrically equivalent $(-1, 1)$ and $(1, 1)$ peaks one obtains:

$$I_{1-1} = I_{11} = 1 + \cos\left(2\pi + \frac{2\pi\Delta}{d}\right) = 1 + \cos\left(\frac{2\pi\Delta}{d}\right). \tag{8}$$
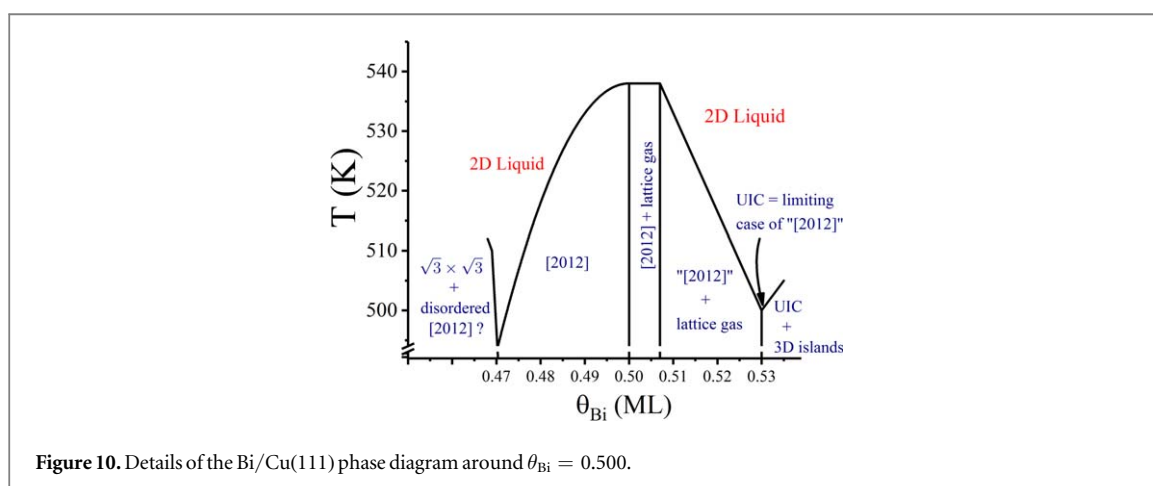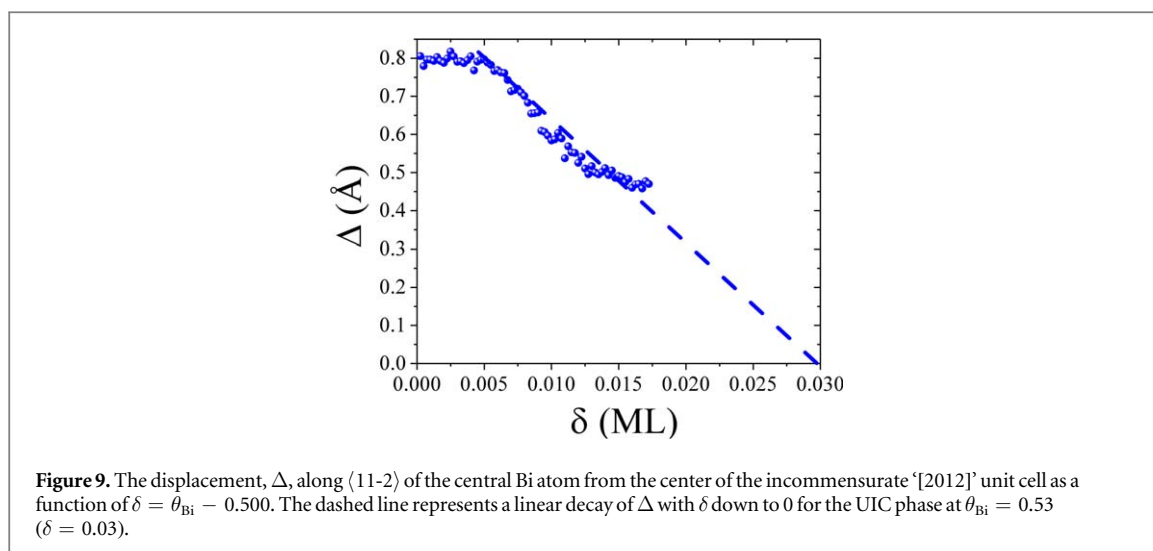
For the relative intensity we then find:

$$\frac{I_{10}}{I_{11}} = \tan^2\left(\frac{\pi\Delta}{d}\right). \tag{9}$$

Possible effects due to diffuse scattering of electrons by the lattice gas [15] are nicely canceled out. Since we deliberately misaligned the microscope to distinguish rotational domains, symmetrically equivalent peaks have different intensities even within a single domain. Therefore, we used the *average* intensity of the two nearest allowed peaks (I_{1-1} and I_{11}) to normalize the intensity of the 'forbidden' peak (I_{10}). To obtain information on Δ (red domain, see figure 2) we take $2 \cdot I_{10}/[I_{1-1} + I_{11}]$ and find $\Delta = 0.80$ Å for the [2012] phase. This value is compared with the previously obtained value of 0.54 Å [8]. The latter was obtained at room temperature and we attribute this difference to a calculated density difference of thermally excited vacancies of about 0.8%. Note that an increase of the density with 0.008 would lead to a decrease of Δ by about 0.25 Å and the resulting Δ-values agree nicely. We are able to monitor the variation of Δ as a function of the compression ξ too. The result is shown in figure 9. For the split peak we integrate over the total profile. For statistical reasons we choose to use peaks for the red domain from figure 2.

Initially, Δ stays constant in line with the build-up of the lattice gas phase (see figure 3 and the corresponding discussion). Immediately upon the set-in of the compression at $\delta \approx 0.0075$ (see figure 3) Δ starts to decrease. It seems to follow a linear decay down to $\Delta = 0$ for the limiting case UIC at $\theta_{Bi} = 0.53$ ($\delta = 0.03$). The dashed line is plotted as a guide to the eye to illustrate this behavior. The continuous decrease of Δ with increasing compression is again in line with the presence of a single '[2012]' phase in the considered θ_{Bi} range.

The current results give rise to a modification of the phase diagram for Bi/Cu(111) around $\theta_{Bi} = 0.500$. The actual result is shown in figure 10.

Figure 9. The displacement, Δ, along $\langle 11\text{-}2 \rangle$ of the central Bi atom from the center of the incommensurate '[2012]' unit cell as a function of $\delta = \theta_{Bi} - 0.500$. The dashed line represents a linear decay of Δ with δ down to 0 for the UIC phase at $\theta_{Bi} = 0.53$ ($\delta = 0.03$).

Figure 10. Details of the Bi/Cu(111) phase diagram around $\theta_{Bi} = 0.500$.

Conclusions

We have carefully calibrated the Bi coverage on Cu(111) using low energy electron microscopy. A [2012] Bi phase is formed with a coverage around the ideal 0.5 ML (1 Bi per 2 Cu outermost layer atoms). Unilateral compression along the close packed direction occurs for $\theta_{Bi} > \frac{1}{2}$. The melting temperature of this phase *increases* with θ_{Bi} for $\theta_{Bi} < 0.5$ and *decreases* for $\theta_{Bi} > \frac{1}{2}$. This remarkable behavior is rationalized by introducing a critical vacancy fraction θ_{vcr} at the melting temperature. This critical fraction is argued to amount to $\theta_{vcr} = 0.055$ (0.0275 Bi vacancies per Cu(111) surface-layer). The corresponding vacancy formation energy is 264 meV at $\theta_{Bi} = 0.500$. The rise of the melting temperature with θ_{Bi} for $\theta_{Bi} < 0.5$ is caused by a continuously decreasing fraction of non-thermal vacancies, while a falling melting temperature for $\theta_{Bi} > 0.5$ is associated with a decreasing vacancy formation energy with increasing compression. The occurrence of a critical vacancy concentration for melting in 2D bears a distinct analogy with the 3D case and the thoughtful consideration of such analogies may well lead to a better understanding of melting in 2D.

The current *in situ* measurements demonstrate the presence of a single and compressed '[2012]' phase for $\theta_{Bi} > 0.500$, at least for temperatures above 410 K. The central Bi atom in the '[2012]' unit cell moves systematically towards the center of the unit cell with increasing uniaxial compression. We find no evidence for the coexistence of two phases, [2012] and UIC as concluded previously from room temperature experiments.

ORCID iDs

Harold J W Zandvliet ⓘ https://orcid.org/0000-0001-6809-139X

References

[1] Strandburg K J 1988 *Rev. Mod. Phys.* **60** 161
[2] Gasser U, Eisenmann C, Maret G and Keim P 2010 *Chem. Phys. Chem* **11** 963
[3] Dillmann P, Maret G and Keim P 2012 *J. Phys.: Condens. Matter* **24** 464118
[4] Sun X, Ma Y L and Zhang Z 2016 *Sci. Rep.* **6** 24056
[5] van Gastel R, Kaminski D, Vlieg E and Poelsema B 2014 *Phys. Rev. B* **89** 075431
[6] van Gastel R, Kaminski D, Vlieg E and Poelsema B 2012 *Phys. Rev. Lett.* **109** 195501
[7] van Gastel R, Kaminski D, Vlieg E and Poelsema B 2009 *Surf. Sci.* **603** 3292
[8] Kaminski D, Poodt P, Aret E, Radenovic N and Vlieg E 2005 *Surf. Sci.* **575** 233
[9] Kaminski D, Poodt P, Aret E, Radenovic N and Vlieg E 2006 *Phys. Rev. Lett.* **96** 056102
[10] Delamare F and Rhead G E 1973 *Surf. Sci.* **35** 185
[11] Linke U and Poelsema B 1985 *J. Phys. E: Sci. Instrum.* **18** 26
[12] Becker A F, Rosenfeld G, Poelsema B and Comsa G 1993 *Phys. Rev. Lett.* **70** 477
[13] Röder H, Schuster R, Brune H and Kern K 1993 *Phys. Rev. Lett.* **71** 2086
[14] Tersoff J 1995 *Phys. Rev. Lett.* **74** 434
[15] Schwarz D, van Gastel R, Zandvliet H J W and Poelsema B B 2012 *Phys. Rev. Lett.* **109** 016101
[16] Kraftmakher Y 1998 *Phys. Rep.* **299** 79 and references therein
[17] Poelsema B, Hannon J B, Bartelt N C and Kellogg G L 2004 *Appl. Phys. Lett.* **84** 2551
[18] Grey F, Feidenhans'l R, Pedersen J S and Nielsen M 1990 *Phys. Rev. B* **41** 9519
[19] Reedijk M F, Arsic J, Kaminski D, Poodt P, van Kessel J W M, Szweryn W J, Knops H and Vlieg E 2003 *Phys. Rev. Lett.* **90** 56104
[20] Lide D R (ed) 2006 *CRC Handbook of Chemistry and Physics* (Boca Raton, FL: CRC Press)
[21] Matsuno N 1977 *J. Phys. Soc. Japan.* **42** 1675
[22] Polatoglou H M, Methfessel M and Scheffler M 1993 *Phys. Rev. B* **48** 1877
[23] Baxter R J 1999 *Ann. Comb.* **3** 191
[24] Müller B H, Schmidt T and Henzler M 1997 *Surf. Sci.* **376** 123